Altered Small-World Brain Functional Networks in Children With Attention-Deficit/Hyperactivity Disorder

Liang Wang,[1,2] Chaozhe Zhu,[2]* Yong He,[3] Yufeng Zang,[2]* QingJiu Cao,[4] Han Zhang,[2] Qiuhai Zhong,[1] and Yufeng Wang[4]

[1]*School of Information Science and Technology, Beijing Institute of Technology, Beijing 100081, People's Republic of China*
[2]*State Key Laboratory of Cognitive Neuroscience and Learning, Beijing Normal University, Beijing 100875, People's Republic of China*
[3]*McConnell Brain Imaging Centre, Montreal Neurological Institute, McGill University, Montreal, Quebec, Canada H3A 2B4*
[4]*Institute of Mental Health, Peking University, Beijing 100083, People's Republic of China*

◆ ━━━━━━━━━━━━━━━━━━━━━━━━━━━━━━━━ ◆

Abstract: In this study, we investigated the changes in topological architectures of brain functional networks in attention-deficit/hyperactivity disorder (ADHD). Functional magnetic resonance images (fMRI) were obtained from 19 children with ADHD and 20 healthy controls during resting state. Brain functional networks were constructed by thresholding the correlation matrix between 90 cortical and subcortical regions and further analyzed by applying graph theoretical approaches. Experimental results showed that, although brain networks of both groups exhibited economical small-world topology, altered functional networks were demonstrated in the brain of ADHD when compared with the normal controls. In particular, increased local efficiencies combined with a decreasing tendency in global efficiencies found in ADHD suggested a disorder-related shift of the topology toward regular networks. Additionally, significant alterations in nodal efficiency were also found in ADHD, involving prefrontal, temporal, and occipital cortex regions, which were compatible with previous ADHD studies. The present study provided the first evidence for brain dysfunction in ADHD from the viewpoint of global organization of brain functional networks by using resting-state fMRI. *Hum Brain Mapp* *30:638–649, 2009.* © 2008 Wiley-Liss, Inc.

Key words: ADHD; connectivity; efficiency; functional magnetic resonance imaging; networks; resting-state; small-world

◆ ━━━━━━━━━━━━━━━━━━━━━━━━━━━━━━━━ ◆

INTRODUCTION

Attention-deficit/hyperactivity disorder (ADHD), as one of the most commonly diagnosed childhood neurobehavioral disorders, is characterized by developmentally inappropriate symptoms of excessive inattention, impulsivity, and hyperactivity [American Psychiatric Association, 1994]. Arising in childhood and persisting into adolescence and adulthood [Faraone et al., 2003], ADHD affects ˜3–5% of school-age children [Spencer et al., 1998]. Children with ADHD have difficulties controlling their behaviors or focusing their attentions which result in an adverse effect on academic performance and social function.

Structural and functional neuroimaging studies have shown that the pathophysiology of ADHD is associated with regional abnormalities involving frontal, parietal, temporal, occipital, and subcortical regions [Bush et al., 2005; Seidman et al., 2004, 2005]. The involved regions have been identified as the components of various functional networks, such as fronto-striatal [Castellanos et al., 2006], fronto-parietal [Dickstein et al., 2006], and fronto-temporal-parietal circuits [Smith et al., 2006]. The regional abnormality may be associated with the dysfunction of the corresponding networks [Bush et al., 2005; Seidman et al., 2004]. Moreover, recent neuroimaging studies have found that ADHD patients showed anatomical [Ashtari et al., 2005; Hill et al., 2003; Hynd et al., 1991; Semrud-Clikeman et al., 1994] and functional [Castellanos et al., in press; Murias et al., 2007; Tian et al., 2006] connectivity abnormalities involving frontal and subcortical regions. Although there are extensive researches on ADHD-related abnormalities in widespread regions and the connectivity, very few studies have yet investigated the topological organization of functional networks in the whole brain in ADHD.

Recent advances in graph theoretical approaches have allowed us to characterize topological properties of complex networks. Using these approaches, Watts and Strogatz [1998] have shown that graphs with densely local connections and few long connections can be characterized as small-world networks. Such a topology has been demonstrated in many complex networks, including social, economical, and biological networks [for a review, see Boccaletti et al., 2006]. Moreover, several recent studies have demonstrated the small-world topology in large-scale structural [Hagmann et al., 2007; He et al., 2007; Hilgetag et al., 2000; Sporns and Zwi, 2004] and functional [Achard et al., 2006; Bassett et al., 2006; Ferri et al., 2007; Micheloyannis et al., 2006a; Salvador et al., 2005a; Stam, 2004; Stephan et al., 2000] brain networks in humans and nonhuman primates. There is also increasing evidence that the small-world properties of brain networks are affected by normal aging [Achard and Bullmore, 2007] and brain diseases, such as schizophrenia [Micheloyannis et al., 2006b], Alzheimer's disease [Stam et al., 2007], epilepsy [Ponten et al., 2007], spinal cord injury [De Vico Fallani et al., 2007], and brain tumor [Bartolomei et al., 2006]. Small-world is an attractive model for the description of complex brain networks, since it provides a quantitative insight into relevant network parameters governing fundamental organization of the brain. In the current study, we hypothesize that the small-world properties of brain functional networks would be altered in children with ADHD.

To test this hypothesis, we used functional magnetic resonance imaging (fMRI) to construct brain functional networks of both ADHD children and normal controls during the resting state. The spontaneous low-frequency fluctuation (LFF) measured by resting-state fMRI is highly synchronous between different brain regions and is physiologically meaningful [Achard and Bullmore, 2007; Achard et al., 2006; Biswal et al., 1995; Fox et al., 2005; Greicius et al., 2003; Jiang et al., 2004; Kiviniemi et al., 2000, 2004; Seeley et al., 2007]. Moreover, recent studies have suggested that the LFF can be employed to characterize the pathophysiological changes of brain disorders [Anand et al., 2005; Cao et al., 2006; Tian et al., 2006; Wang et al., 2006; Greicius et al., 2007; Zang et al., 2007]. In this study, we measured functional connectivity [Friston et al., 1993] by calculating correlations between the time series of any pair of the 90 cortical and subcortical regions of the whole brain during the resting state and then obtained a set of interregional correlation matrices. The resulting correlation matrices were further thresholded into undirected graphs to construct brain functional networks. Finally, the topological properties of the networks were characterized by graph theoretical approaches, and the differences between two groups were further statistically evaluated.

MATERIALS AND METHODS

Participants

A total of 56 children (29 ADHD and 27 control boys) participated in the experiment. All subjects were right-handed and claimed to be in no lifetime history of head trauma with loss of consciousness and neurological illness or other severe psychical disease. All subjects scored intelligence quotient (IQ) of higher than 80 on the Wechsler Intelligence Scale for Chinese Children-Revised Version [Gong and Cai, 1993]. The ADHD patients were recruited from the outpatients of the Institute of Mental Health, Peking University. A structured diagnostic interview, the Clinical Diagnostic Interviewing Scale [Yang et al., 2001], which is based on Diagnostic and Statistical Manual of Mental Disorders, Fourth Edition criteria, was administered to diagnose ADHD. The criteria for ADHD included (1) predominantly inattention type (ADHD-I) or combined type (ADHD-C), (2) no history of emotional disorders, affective disorders, Tourette disorder, and other Axis I psychiatric disorder, (3) no evidence of severe language development delay and communication problems as determined through clinical history, parents interview, and observation of the children. Boys with hyperactivity disorder with comorbid conduct disorder or oppositional defiant disorder were not excluded. Controls were recruited from

local middle school. They were excluded from the diagnosis of ADHD according to Clinical Diagnostic Interviewing Scale [Yang et al., 2001] and had no history of emotional disorders, affective disorder, Tourette disorder, and other Axis I psychiatric disorder. This study was approved by the Research Ethics Review Board of Institute of Mental Health, Peking University. After completing the description of the nature of the procedure, informed consent was obtained from the parents of each subject, and all of the children agreed to participate in this study. Data from 17 subjects were excluded due to excessive motion (see Preprocessing). Data of 19 ADHD and 20 control boys were used in this study (age: Controls 13.32 ± 0.97 years, ADHD 13.59 ± 1.52 years, $t(37) = -0.66$, $P = 0.516$; IQ: Controls 115.25 ± 11.85, ADHD 102.59 ± 8.62, $t(37) = 3.66$, $P < 0.001$).

fMRI Data Acquisition and Preprocessing

All MR images were acquired using a Siemens Trio 3-T scanner (Siemens, Erlangen, Germany) in the Institute of Biophysics, Chinese Academy of Sciences. Each subject lay supine with the head snugly fixed by belt and foam pads to reduce the effects of head movement. A T1-weighted sagittal three-dimensional spoiled gradient-recalled sequence was acquired covering the whole brain: 176 slices, thickness/gap = 1.0/0 mm, matrix = 256 × 256, repetition time = 1,700 ms, echo time = 3.93 ms, flip angle = 15°, field of view = 240 mm × 240 mm. Functional images were collected by using an echo-planar imaging (EPI) sequence: 30 axial slices, thickness/gap = 4.5/0 mm, matrix = 64 × 64, repetition time = 2,000 ms, echo time = 30 ms, flip angle = 90°, field of view = 220 mm × 220 mm. Subjects were instructed to keep their eyes closed, relax their minds, and remain motionless as much as possible during the EPI data acquisition. The scan lasted for 480 s. For each dataset, the first 10 volumes were discarded to allow for T1 equilibration effects and the adaptation of the subjects to the circumstances, leaving 230 volumes for further analysis.

Image preprocessing was carried out using the SPM5 software package (http://www.fil.ion.ucl.ac.uk/spm). All datasets were corrected initially for temporal offsets using the sinc interpolation and head movement-related effects using a six-parameter (rigid body) spatial transformation [Friston et al., 1995]. Data of 17 boys (10 ADHD and 7 controls) with maximum displacement in any direction of larger than 2 mm or head rotation of larger than 1.5° were excluded from further analysis. The resulting datasets were further spatially normalized to Talairach and Tournoux coordinate space [Talairach and Tournoux, 1998] using an optimum 12-parameter affine transformation and nonlinear deformations [Ashburner and Friston, 1999], and then resampled to 3-mm isotropic voxels. Finally, the fMRI data were temporally filtered (0.0083–0.15 Hz) by using an ideal rectangle window filter of the AFNI software [Cox, 1996] to remove low-frequency drift and high-frequency physiological noises [Greicius et al., 2003; Seeley et al., 2007].

Functional Connectivity Matrix and Graph Construction

To measure the functional connectivity among regions, the brain was first parcellated into 90 anatomical regions of interest (45 in. each hemisphere, see Table I) using the anatomical automatic labeling (AAL) template [Tzourio-Mazoyer et al., 2002]. The mean time series of each region was then obtained by averaging the time series of all voxels in the region. Several sources of variance of BOLD signal were further removed from the mean time series using a multiple linear regression model. The regressors consisted of the estimated profiles of head motion (three for translation and three for rotation) and the global brain activity [Fox et al., 2005]. The residuals of this regression were then used to substitute for the raw mean time series of the corresponding regions. Pearson's correlation coefficients between the residual time series of each possible pair of the 90 regions were further computed to produce a symmetric correlation matrix (i.e., functional connectivity matrix) for each subject.

To investigate the properties of brain functional networks, each correlation matrix was thresholded into a binary graph (i.e., network), where nodes represent brain regions and edges represent undirected connections. In this study, network cost was adopted as a threshold measurement since it concisely couples with network efficiency (see the following section for the definition of efficiency measures), thus providing a biologically meaningful description of the performance of a network [Achard and Bullmore, 2007; De Vico Fallani et al., 2007; Latora and Marchiori, 2001]. C_G, the cost of a graph G, is defined in (1)

$$C_G = \frac{K}{N(N-1)/2} \tag{1}$$

where N and K are the total number of nodes and edges in the graph G, respectively. $N(N - 1)/2$ is the number of all the possible edges in the G. C_G measures how expensive it is to build a network. It needs to note that the selection of different cost thresholds may lead to graphs with distinct topologies: high thresholds yield sparser graphs and low thresholds yield denser ones. However, since there is no definitive way currently to select a precise threshold in complex brain networks studies [Achard and Bullmore, 2007; Bassett et al., 2006; He et al., 2007], in the present study, we thus investigated the properties of the networks over a wide range of threshold values. This can allow us to explore the differences in network properties between two groups at each threshold level. Here, the range of cost threshold was set from 0.05 to 0.5 to make (1) the small-world attributes estimable [i.e., the mean degree $\bar{k}$ of the graph is greater than the log of the number

TABLE I. Regions of interest in an entire human brain functional network

Region	Abbrevation	Region	Abbrevation
Precentral gyrus	PreCG	Lingual gyrus	LING
Superior frontal gyrus (dorsal)	SFGdor	Superior occipital gyrus	SOG
Orbitofrontal cortex (superior)	ORBsup	Middle occipital gyrus	MOG
Middle frontal gyrus	MFG	Inferior occipital gyrus	IOG
Orbitofrontal cortex (middle)	ORBmid	Fusiform gyrus	FFG
Inferior frontal gyrus (opercular)	IFGoperc	Postcentral gyrus	PoCG
Inferior frontal gyrus (triangular)	IFGtriang	Superior parietal gyrus	SPG
Orbitofrontal cortex (inferior)	ORBinf	Inferior parietal lobule	IPL
Rolandic operculum	ROL	Supramarginal gyrus	SMG
Supplementary motor area	SMA	Angular gyrus	ANG
Olfactory	OLF	Precuneus	PCUN
Superior frontal gyrus (medial)	SFGmed	Paracentral lobule	PCL
Orbitofrontal cortex (medial)	ORBmed	Caudate	CAU
Rectus gyrus	REC	Putamen	PUT
Insula	INS	Pallidum	PAL
Anterior cingulate gyrus	ACG	Thalamus	THA
Middler cingulate gyrus	MCG	Heschl gyrus	HES
Posterior cingulate gyrus	PCG	Superior temporal gyrus	STG
Hippocampus	HIP	Temporal pole (superior)	TPOsup
Parahippocampal gyrus	PHG	Middle temporal gyrus	MTG
Amygdala	AMYG	Temporal pole (middle)	TPOmid
Calcarine cortex	CAL	Inferior temporal gyrus	ITG
Cuneus	CUN		

The regions are described by Tzourio-Mazoyer et al. (2002), and the abbreviations are provided according to Salvador et al. (2005a) and Achard et al. (2006).

of nodes ($N = 90$); Watts and Strogatz, 1998. Note that $\bar{k}$ is the average of the degree over all nodes, where the degree of a node represents the number of connections to that node], and (2) the resulting matrices have sparse properties. Such a criteria of threshold selection has been utilized in several recent studies [Achard and Bullmore, 2007; Achard et al., 2006; He et al., 2007].

Efficiency of Small-World Networks

For a given binary graph G with a wiring cost C_G, we can evaluate its small-world attributes. Originally, Watts and Strogatz [1998] proposed clustering coefficient (C_p) and shortest path length (L_p) to quantify small-world properties of a network. Recent studies have indicated that, in small-world analysis, efficiency measure has a number of technical and conceptual advantages over conventional C_p and L_p measures, since it provides a single measure to analyze both the local and the global behavior of a network and can also deal with either the disconnected or nonsparse graphs or both [Latora and Marchiori, 2001]. Recently, Achard and Bullmore [2007] applied the efficiency metric for the first time to investigate human brain functional networks. They found that human brain functional networks exhibited economical small-world properties and that the economical performance of these networks was affected by normal aging and a dopamine receptor antagonist. Using the efficiency measures, in this study, we investigated brain functional networks in the ADHD and control boys. Briefly, the efficiency of a graph G in (2) is defined as the inverse of the harmonic mean of

the minimum path length, $L_{i,j}$ (i.e., the shortest length of the path from node i to node j) [Latora and Marchiori, 2001].

$$E(G) = \frac{1}{N(N-1)} \sum_{i \neq j \in G} \frac{1}{L_{i,j}} \qquad (2)$$

According to the definition, $L_{i,j}$ would be infinite if there is no path between node i and node j, thus contributing nothing to the sum. When the graph G represents a whole network, $E(G)$ measures the global efficiency, $E_{glob}(G)$, of the network that quantifies the efficiency of information propagation over it. When considering a subgraph of the whole graph G, such as G_i, which is composed of the nearest neighbors of node i, $E(G_i)$ indicates the efficiency of the subgraph G_i, measuring how efficient the information is exchanged in the subgraph. Thus, the local efficiency, $E_{loc}(G)$, of the whole network is defined in (3) as the average of the efficiency $E(G_i)$ over all subgraphs included in the network [Latora and Marchiori, 2001].

$$E_{loc}(G) = \frac{1}{N} \sum_{i \in G} E(G_i) \qquad (3)$$

Besides the two global metrics, $E_{glob}(G)$ and $E_{loc}(G)$, in this study, we also investigated regional nodal efficiency in (4), $E_{nodal}(G,i)$, defined as the inverse of the harmonic mean of the minimum length of path between node i and all other nodes in a graph [Achard and Bullmore, 2007]. $E_{nodal}(G,i)$ measures the communication efficiency between a node i and all the other nodes in the network G.
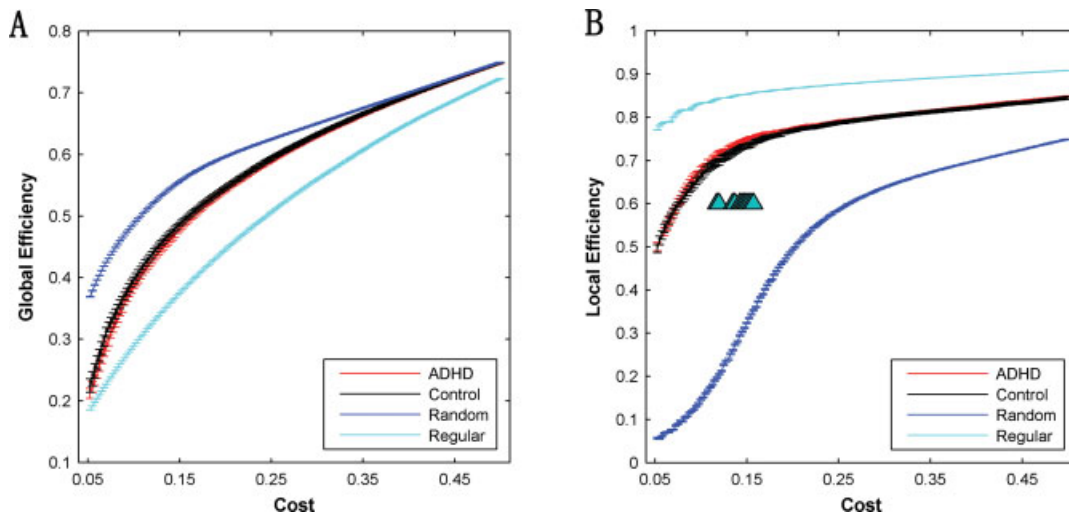
Figure 1.

Small-world properties of brain functional networks. The (**A**) global and (**B**) local efficiency (y-axis) are shown as a function of the cost (x-axis) for random, regular, and brain networks. Error bars denote standard error of the mean for a network type. For each network, the global and local efficiency increase with the cost. The efficiency curves locate between random graphs and regular networks over the entire cost range ($0.05 \leq \cos t \leq$ 0.50, with an incremental interval of 10 edges). There are no significant differences in the global efficiency between the two groups, whereas there are significant differences found in local efficiency at an intermediate range of the cost (0.12–0.16). Color-coded upright triangles indicate significant differences between the two groups (two-sample t-test, $P < 0.05$).

$$E_{\text{nodal}}(G, i) = \frac{1}{N - 1} \sum_{j \in G} \frac{1}{L_{i,j}} \qquad (4)$$

Statistical evaluation of small-world properties requires comparable regular and random networks [Watts and Strogatz, 1998]. In this study, we generated populations of regular networks ($n = 100$) and random graphs ($n = 100$) that preserved the same number of nodes and edges, respectively. The efficiency of G was compared with that of random graphs, G_{rand}, and regular graphs, G_{reg}. The graph G would be considered a small-world if it met the following conditions [Achard and Bullmore, 2007]:

$$E_{\text{glob}}(G_{\text{reg}}) < E_{\text{glob}}(G) < E_{\text{glob}}(G_{\text{rand}}) \text{ and}$$
$$E_{\text{loc}}(G_{\text{rand}}) < E_{\text{loc}}(G) < E_{\text{loc}}(G_{\text{reg}}) \quad (5)$$

In the present study, we also measured the cost efficiency as the difference between global efficiency and cost, i.e., $E_{\text{glob}}(G) - C_G$, which would be positive in the case of an economical network [Achard and Bullmore, 2007].

Statistical Analysis

In the present study, we first performed a lilliefors test (MATLAB Statistics Toolbox, The MathWorks, Natick, MA) to verify whether the small-world parameters (E_{glob}, E_{loc}, and E_{nodal}) followed a normal distribution [Conover, 1980]. According to the hypothesis-test results, the data had a normal distribution over the selected cost range.

Then, we compared the global metrics (E_{glob} and E_{loc}) at each cost value to evaluate the small-world topological differences between the two groups using a two-sample t-test. In addition, between-group difference in nodal efficiency of each region was also tested by a two-sample t-test at a given cost.

RESULTS

Small-World Brain Functional Networks in Children

Figure 1 illustrates the global and local efficiencies of the random, regular, and brain networks of both the groups (ADHD and control) as a function of cost.

We found that the global efficiency was higher in the random graphs than that in the corresponding regular networks (Fig. 1A), but the local efficiency was higher in the regular networks than that in the corresponding random graphs (Fig. 1B). Furthermore, we found that the efficiency curves of brain networks of both the groups located between the curves of the random and regular graphs in a wide range of cost, suggesting small-world architectures in the brain functional networks. Additionally, we also observed that the cost efficiency (i.e., $E_{\text{glob}} - C_G$) of brain networks of both groups were greater than zero over the whole range of cost threshold (see Fig. 2) and had a maximum positive value at an approximate cost of 0.20 (Fig. 2, black arrows), suggesting economical properties in brain
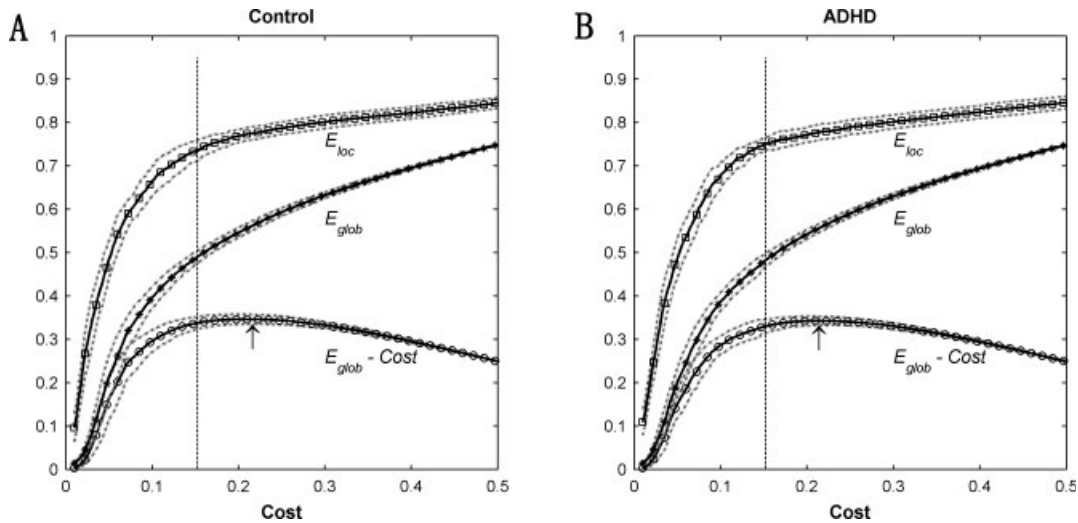
Figure 2.

Economical properties of brain functional networks. The global (i.e., E_{glob}) and local efficiency (i.e., E_{loc}) of brain networks in both controls and ADHD groups increase monotonically with the cost. The cost efficiency (the difference between the global efficiency and cost, i.e., $E_{glob} - C_G$) has a maximum value at the cost of 0.2 (the black arrows). The broken lines denote plus and minus one standard error of the mean corresponding to network parameters. The vertical lines denote the cost of 0.15, associated with the sparse networks used in Fig. 3 through Fig. 6.

networks. These results are consistent with a recent study [Achard and Bullmore, 2007].

Altered Small-World Topology of Brain Functional Networks in ADHD

At a wide range of cost threshold, the brain networks of the ADHD group demonstrated decreased global efficiency and increased local efficiency compared with controls (see Fig. 1). Statistical analysis further revealed that there were no significant differences in global efficiency between the two groups (Fig. 1A), whereas there were significantly different ($P < 0.05$) in local efficiency at a range of cost (0.12 < cost < 0.16) (Fig. 1B, upright triangles). Furthermore, we found that, at a cost of 0.15, there was the most significant between-group difference ($P = 0.016$) in the local efficiency and there was a decreased trend in the global efficiency of functional network in ADHD ($P = 0.144$) (see Fig. 3). The patterns of the changes in the network efficiency in ADHD reflect the tendency of a disorder-related shift toward regular networks.

Altered Nodal Efficiency in ADHD

To further reveal the influence of the disorder on regionally nodal characteristics of the brain networks, the group difference in nodal efficiency was tested at the cost of 0.15 corresponding to the maximal between-group difference in the local efficiency. We found that ADHD patients demonstrated significant decreases in nodal efficiency in the medial prefrontal, temporal, and occipital cortex regions

(see Fig. 4) and increases in the inferior frontal cortex and subcortical regions (see Fig. 4; Table II). Our results suggest that the nodal efficiency of brain functional networks is profoundly affected by ADHD. To highlight the affected
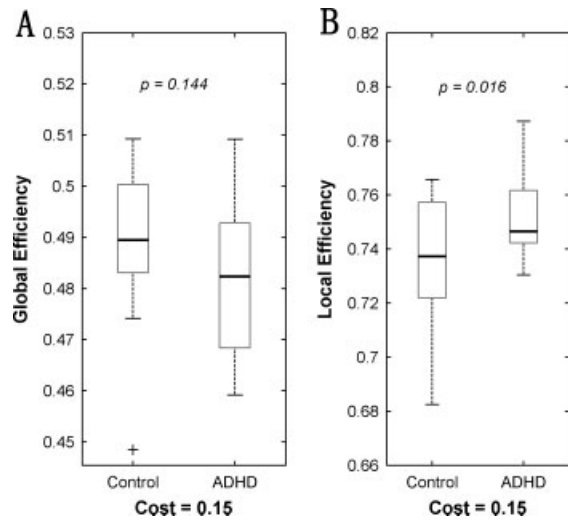

Figure 3.

Box-plots showing median, interquartile, and range for global efficiency (**A**) and local efficiency (**B**) in each group at the cost of 0.15. P values correspond to the significant level by means of a two-sample t-test. Note that there is an outlier (black plus sign) in the E_{glob} of the control group. There would be significantly different in the E_{glob} ($P = 0.039$) and E_{loc} ($P = 0.026$) between the two groups if this outlier is removed.
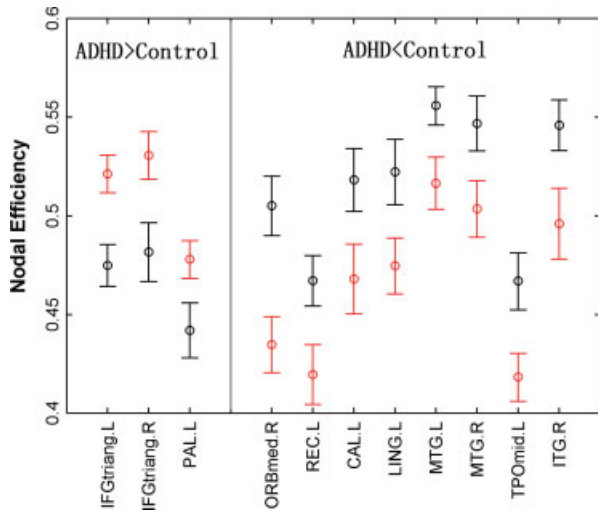
Figure 4.

ADHD-related changes in nodal efficiency at the cost of 0.15. Red and black error bars correspond to the mean and standard error of the mean for the ADHD and control group, respectively. See Table II for the details of the regions. See Table I for the abbreviations of the regions.

brain regions, the whole brain topological map was mapped into anatomical space for one control (Fig. 5A) and one ADHD subject (Fig. 5B).

The Relation Between Network Efficiency and IQ

In order to evaluate the potential effect of IQ on our results, we examined the correlations between the topolog-

TABLE II. Regions showing significant changes in nodal efficiency in ADHD (cost = 0.15)

Region	Hemisphere	t value	P value
Decreased nodal efficiency in ADHD			
Orbitofrontal cortex (medial)	R	3.41	0.001
Rectus gyrus	L	2.38	0.022
Lingual gyrus	L	2.18	0.035
Calcarine cortex	L	2.10	0.042
Middle temporal gyrus	L	2.37	0.023
	R	2.16	0.037
Inferior temporal gyrus	R	2.24	0.032
Temporal pole (middle)	L	2.22	0.033
Increased nodal efficiency in ADHD			
Inferior frontal gyrus (triangle)	L	−3.26	0.002
	R	−2.57	0.014
Pallidum	L	−2.16	0.038

t, statistical value showing nodal difference ($P < 0.05$) between two groups (positive t-value means decreased nodal efficiency in the ADHD group); R, right; L, left.

ical parameters (E_{glob}, E_{loc}, and E_{nodal}) and IQ within each group. We found that, although there was significant group difference in IQ, the correlation was not significant between the IQ scores and the global efficiency (ADHD: $r = 0.296$, $P = 0.249$; Controls: $r = 0.027$, $P = 0.911$) or the local efficiency (ADHD: $r = 0.014$, $P = 0.959$; Controls: $r = 0.061$, $P = 0.797$) values within each group. There were also no significant correlations between the IQ and nodal efficiency of brain regions showing significantly between-group difference except the left lingual gyrus in the ADHD group ($r = 0.633$, $P = 0.006$).
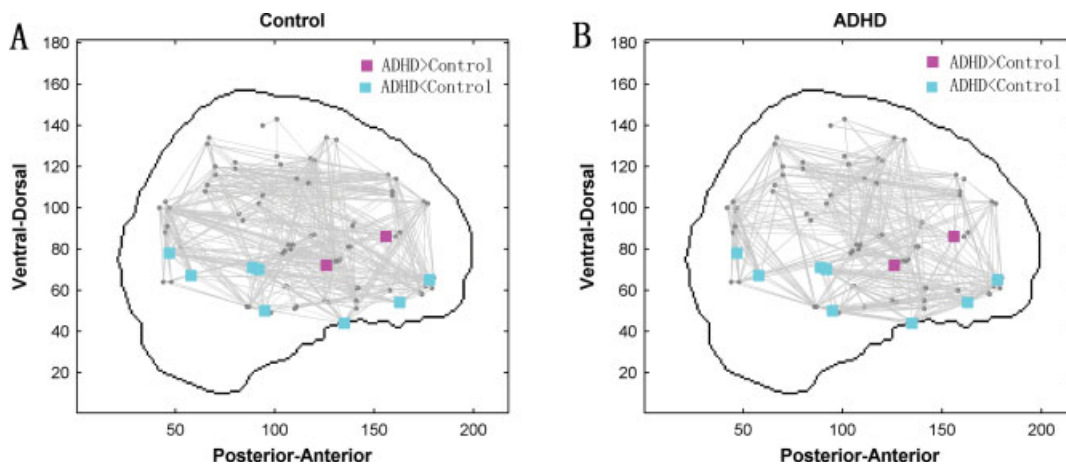

Figure 5.

ADHD-related changes in nodal efficiency in topological maps. The networks were constructed by converting the individual correlation matrices to generate sparse networks with the cost of 0.15 (the vertical lines in Fig. 2) and shown in a sagittal view of the brain. These black dots represent the brain regions that were visualized by locating their y and z centroid coordinates in the anatomical space. Cyan and magenta squares show significantly lower and higher nodal efficiency of brain regions in the ADHD patients compared with the controls, respectively. See Table II for the details of the regions.

DISCUSSION

This is the first study, to our knowledge, to investigate small-world properties of brain functional networks in children with and without ADHD. We found that brain functional networks exhibited economical small-world topology in both groups. An altered functional network, however, was found in the brain of ADHD. In particular, a tendency of shift toward regular networks was demonstrated in ADHD when compared with normal controls. Moreover, our study revealed that nodal efficiency was profoundly affected at several regions of prefrontal, temporal, and occipital cortices, which were compatible with previous studies in ADHD. Our results suggested that the widely distributed functional brain networks are altered in ADHD, thus providing further evidence for brain dysfunction associated with this disease [Bush et al., 2005; Seidman et al., 2004].

Since small-world networks were quantitatively described by Watts and Strogatz [1998], human brain functional networks with a small-world configuration have been validated by using various imaging techniques, such as MEG, EEG, and fMRI [for reviews, see Bassett and Bullmore, 2006; Stam and Reijneveld, 2007]. In agreement with these previous findings, in the present study, we also observed the features of small-world architecture in the functional brain networks in children both with and without ADHD using the resting-state fMRI (see Fig. 1), thus providing further support for the opinion that small-world brain networks have the ability to display tolerance in the face of developmental aberration or disease [Achard et al., 2006]. Moreover, the functional networks with small-world features were also found to show economical properties (see Fig. 2), consistent with previous studies [Achard and Bullmore, 2007]. Together, these findings supported the standpoint that brain networks might have been evolved to maximize cost efficiency of parallel information processing, i.e., high efficiency of parallel information transfer at low cost [Kaiser and Hilgetag, 2006; Sporns et al., 2004].

Although both of ADHD and control groups had economical small-world properties as elucidated earlier, the topology of the ADHD group was altered compared to the control group. A tendency of decreased global efficiency of the brain networks was found in ADHD over the whole cost range. It has been suggested that the global efficiency is affected by the loss of long-range connections [Latora and Marchiori, 2001]. Structural and diffusion imaging studies found that the regions showing the ADHD-related abnormality are associated with long fibers in ADHD children, such as the corpus callosum (connecting the left and right cerebral hemispheres) [Hill et al., 2003; Hynd et al., 1991; Semrud-Clikeman et al., 1994] and the anterior limb of internal capsule (containing thalamocortical fibers and corticopontine fibers) [Ashtari et al., 2005]. The abnormalities may incur the disruption to the long-range communication among parts of the brain. A recent research has also indicated abnormal long-range connections (dorsal anterior cingulate and medial parietal lobe) in ADHD [Castellanos

et al., in press]. All these abnormalities may contribute to the decreasing tendency of global efficiency of brain network in ADHD. In the current study, significantly increased local efficiency of the brain networks was also found in ADHD children compared to the controls. The underlying mechanisms of increased local efficiency of a network have been widely discussed in various studies. For example, De Vico Fallani et al. [2007] reported that increased local efficiency in spinal cord injured patients could be attributable to a functional reorganization (i.e. brain plasticity). Latora and Marchiori [2001] indicated that the higher the local efficiency of a network, the larger fault tolerance was the network at the face of external attack. We thus suspected that the higher value of local efficiency in ADHD observed here might suggest a kind of defense mechanism responsible for suppressing the disorder affection.

Although both the ADHD children and controls showed small-world attributes in their brain functional networks, the increased local efficiency combined with slightly decreased global efficiency made their networks topology exhibit the tendency of a shift toward regular networks (see Fig. 1). It has been suggested that the small-world structure reflects an optimal balance between local processing and global integration [Sporns and Tononi, 2002]. Therefore, any abnormal shift caused by brain diseases toward either random [Bartolomei et al., 2006; Micheloyannis et al., 2006b; Ponten et al., 2007] or regular [De Vico Fallani et al., 2007] networks may reflect a less optimal network organization. Though the biological causes of underlying the shift remain still unclear, the regular configurations in complex networks have been found to demonstrate low global coordination and slow information flow compared to small-world arrangements [Barahona and Pecora, 2002; Lago-Fernandez et al., 2000; Nishikawa et al., 2003; Strogatz, 2001]. Hence, our results suggested that the ADHD-related network shift may reflect the abnormalities of network architecture.

As described by Achard and Bullmore [2007], the nodal efficiency measures the extent to which the node connects all other nodes of a network, which may indicate the importance of the nodal area in the whole brain network. Using this measure, we here found abnormal nodal efficiency in several regions, involving the prefrontal, temporal, occipital, and subcortical regions (Table II) that were, in general, concerned in ADHD studies. The orbital frontal cortex (OFC) is associated with executive function network [Makris et al., 2007]. The decreased nodal efficiency in the OFC was in accordance with several structural and functional imaging studies that have found cortical atrophy and reduced activity in this region in the ADHD patients [Lee et al., 2005; Makris et al., 2007], which might suggest the abnormalities of executive function in the patients. In addition, several regions belonging to temporal and occipital cortices were also found to have significant decreases in nodal efficiency (Table II), which were compatible with previous studies showing ADHD-related structural and functional abnormalities in these regions [Castellanos
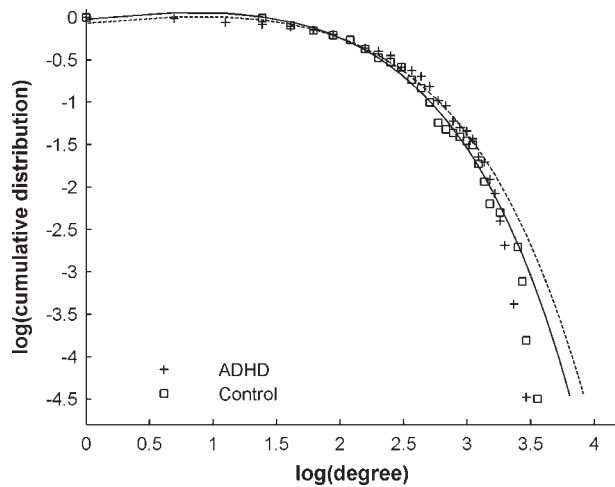
Figure 6.

The degree distributions of human brain functional networks at the cost of 0.15. The degree distribution of both the ADHD (solid line) and control (broken line) subject can be well fitted by an exponentially truncated power-law form ($P(k) \sim k^{a-1} e^{k/k_c}$, where a is an estimated exponent and k_c is a cutoff degree) in the log–log plot. Plus signs and open squares denote the data points in the ADHD (α = 1.266, k_c = 9.060) and the control (α = 1.266, k_c = 7.914), respectively. Note that there are no significant differences in α ($t(37)$ = 0.412, P = 0.683) and k_c ($t(37)$ = −0.141, P = 0.889) between the two groups.

et al., 2002; Durston et al., 2004; Schulz et al., 2004]. In contrast, the inferior frontal gyrus (IFG) exhibited significantly increased nodal efficiency. The IFG was critical for response inhibition [Aron et al., 2003], dysfunction of which has been considered as the core deficit in ADHD [Barkley, 1997; Schulz et al., 2004; Vaidya et al., 1998]. The greater nodal efficiency may thus reflect greater inhibitory effort in the ADHD children. Together, our findings of ADHD-related changes in the nodal efficiency reported here suggest that the nodal roles in brain functional networks are profoundly affected by this disorder.

In addition to the efficiency measures aforementioned, in this study, we also investigated the degree distribution of brain functional networks of both the ADHD and controls groups. Our results demonstrated that the brain networks of both groups followed a truncated power-law form ($P(k) \sim k^{a-1} e^{k/k_c}$, where a is an estimated exponent and k_c is a cutoff degree) as opposed to scale-free regime (see Fig. 6), consistent with previous studies [Achard et al., 2006; He et al., 2007]. Further statistical analysis indicated that there were no significant difference in the fitted parameters [a: $t(37)$ = 0.412, P = 0.683; k_c: $t(37)$ = −0.141, P = 0.889] between the two groups, implying that the degree distribution property of brain functional networks was not altered by this disorder. The truncated power-law distribution shown here suggests that the human brain network includes some core regions but prevents the appearance of the huge hubs with

many connections. Such a network structure has been demonstrated to be more resilient to targeted attacks, but equally resilient to random errors as compared to a scale-free network [Achard et al., 2006; Albert et al., 2000]. Although physical constraints may account for the form of this degree distribution, it remains still unclear about the biological causes underlying this network topology and would be meaningful to further clarify the issue in future studies.

In the present study, although IQ scores between two groups was significantly different, no significant correlations were found between IQ and the global, local, and nodal efficiency within each group, except the left lingual gyrus in the ADHD group. The result indicated that our finding of altered network efficiency in ADHD might not be accounted for by the IQ scores. However, using an EEG technique, Micheloyannis et al. [2006a] reported that the IQ was correlated with the topological parameters of brain networks during working memory tasks. Nonetheless, they did not find significant correlations during the no-task or rest condition, consistent with the current study. These results suggest that the topology of brain networks during the rest state is greatly distinct from that during the task state. Future studies might be helpful to further clarify the relation between IQ and network topology.

Several issues need to be further addressed. First, in order to construct functional brain networks, the present study used a prior template (AAL) to parcellate the whole brain into 90 regions. Although such a template has been applied to several recent studies [Achard and Bullmore, 2007; Achard et al., 2006; Salvador et al., 2005a, 2005b], different parcellation schemes may affect our results. In future studies, other available templates [He et al., 2007; Toga et al., 2006] could be adopted to explore the effect of the templates on the networks architectures. Second, a wide range of cost thresholds were employed to investigate network efficiency, and results without correction were reported in this work. As discussed in the method section, different thresholds may lead to graphs with distinct topologies, but no definitive approach is available to determine a single precise threshold so far. Thus, the use of the wide range of thresholds is reasonable for this preliminary study. Moreover, while uncorrected results were reported here, the present study provided a meaningfully specific cost range (0.1–0.15) that could be employed in future to reduce the problem of multiple comparisons. In addition, the use of a large number of samples would be also important to increase the statistical power. Third, in this study, the brain functional networks were constructed based on the thresholded correlation matrices. It is also possible to construct the brain networks with continuous weighting that provides more detailed connectivity information between network nodes compared with the binary graphs [Achard and Bullmore, 2007; Barrat et al., 2004; Jiang et al., 2004; Latora and Marchiori, 2001]. However, the weighted models could lead to the complications of statistical features descriptions in graph theoretical analysis, thus the initial study confined itself to a simple binary

connectivity analysis. In future studies, it would be interesting to apply efficiency and cost measurements to the weighted networks and further investigate their topological properties in ADHD. Fourth, in this work we used resting-state fMRI to investigate brain functional networks. Previous work has suggested that spontaneous LFFs measured by BOLD fMRI probably reflect underlying anatomical connectivity of the cortex [Achard et al., 2006; Salvador et al., 2005a]. For example, in macaque cortex, Honey et al. [2007] have demonstrated that spontaneous neuronal dynamics at multiple temporal scales can be related to underlying anatomical connectivity. In human cortex, He et al. [2007] have also demonstrated that the structural brain networks constructed from cortical thickness data exhibit topological and anatomical similarity with the low-frequency brain functional networks. Therefore, we suspected that the ADHD-associated changes in topological organization found in this study may reflect the abnormality in structural brain networks in patients, which needs to be further studied in future. Finally, our results could be potentially influenced by the preprocessing approaches used in this study. To date, however, no systematic study is conducted to evaluate the effects of the preprocessing approaches on graphic properties. Nevertheless, there were evidences for the effect of frequency band on the graphs. For example, Salvador et al. [2005b, 2008] demonstrated that resting-state functional connectivity between regions was related to specific frequency intervals: low-frequency components associated with long-distance connections and high-frequency with short-distance connections. Achard et al. [2006] also reported that brain functional networks exhibited small-world properties at multiple time scales, but most salient in the low-frequency interval (0.03–0.06 Hz). In the current study, we also investigated topological parameters of brain functional networks constructed by time series of other frequency band (lower than 0.0083 Hz or higher than 0.15 Hz) and found that there were no significant differences in E_{glob}, E_{loc} and E_{nodal} between the two groups. In future studies, it would be important to systematically analyze the effects of different preprocessing procedures on the topological properties of brain networks.

In summary, this is the first study to reveal the topological properties of brain functional networks in children with ADHD using the resting-state fMRI. Our results provided further support for the presence of small-world features in complex brain networks, and more importantly, we found that the disorder had a deleterious effect on the topological organization of brain functional networks. These findings were compatible with previous ADHD studies from structural and functional imaging, thus enhancing our understanding of the underlying pathophysiology of ADHD and discriminating the neuropathological state of mental disorders.

ACKNOWLEDGMENTS

REFERENCES

Achard S, Bullmore E (2007): Efficiency and cost of economical brain functional networks. PLoS Comput Biol 3:e17.

Achard S, Salvador R, Whitcher B, Suckling J, Bullmore E (2006): A resilient, low-frequency, small-world human brain functional network with highly connected association cortical hubs. J Neurosci 26:63–72.

Albert R, Jeong H, Barabasi AL (2000): Error and attack tolerance of complex networks. Nature 406:378–382.

American Psychiatric Association (1994): Diagnostic and Statistical Manual of Mental Disorders,4th ed. Washington, DC: American Psychiatric Press.

Anand A, Li Y, Wang Y, Wu J, Gao S, Bukhari L, Mathews VP, Kalnin A, Lowe MJ (2005): Activity and connectivity of brain mood regulating circuit in depression: A functional magnetic resonance study. Biol Psychiatry 57:1079–1088.

Aron AR, Fletcher PC, Bullmore ET, Sahakian BJ, Robbins TW (2003): Stop-signal inhibition disrupted by damage to right inferior frontal gyrus in humans. Nat Neurosci 6:115–116.

Ashburner J, Friston KJ (1999): Nonlinear spatial normalization using basis functions. Hum Brain Mapp 7:254–266.

Ashtari M, Kumra S, Bhaskar SL, Clarke T, Thaden E, Cervellione KL, Rhinewine J, Kane JM, Adesman A, Milanaik R, Maytal J, Diamond A, Szeszko P, Ardekani BA (2005): Attention-deficit/hyperactivity disorder: A preliminary diffusion tensor imaging study. Biol Psychiatry 57:448–455.

Barahona M, Pecora LM (2002): Synchronization in small-world systems. Phys Rev Lett 89:054101.

Barkley RA (1997): Behavioral inhibition, sustained attention, and executive functions: constructing a unifying theory of ADHD. Psychol Bull 121:65–94.

Barrat A, Barthelemy M, Pastor-Satorras R, Vespignani A (2004): The architecture of complex weighted networks. Proc Nat Acad Sci USA 101:3747–3752.

Bartolomei F, Bosma I, Klein M, Baayen JC, Reijneveld JC, Postma TJ, Heimans JJ, van Dijk BW, de Munck JC, de Jongh A, Cover KS, Stam CJ (2006): Disturbed functional connectivity in brain tumour patients: Evaluation by graph analysis of synchronization matrices. Clin Neurophysiol 117:2039–2049.

Bassett DS, Bullmore E (2006): Small-world brain networks. Neuroscientist 12:512–523.

Bassett DS, Meyer-Lindenberg A, Achard S, Duke T, Bullmore E (2006): Adaptive reconfiguration of fractal small-world human brain functional networks. Proc Natl Acad Sci USA 103:19518–19523.

Biswal B, Yetkin FZ, Haughton VM, Hyde JS (1995): Functional connectivity in the motor cortex of resting human brain using echo-planar MRI. Magn Reson Med 34:537–541.

Boccaletti S, Latora V, Moreno Y, Chavez M, Hwang D (2006): Complex networks: structure and dynamics. Phys Reports 424:175–308.

Bush G, Valera EM, Seidman LJ (2005): Functional neuroimaging of attention-deficit/hyperactivity disorder: A review and suggested future directions. Biol Psychiatry 57:1273–1284.

Cao Q, Zang Y, Sun L, Sui M, Long X, Zou Q, Wang Y (2006): Abnormal neural activity in children with attention deficit hyperactivity disorder: A resting-state functional magnetic resonance imaging study. Neuroreport 17:1033–1036.

Castellanos FX, Lee PP, Sharp W, Jeffries NO, Greenstein DK, Clasen LS, Blumenthal JD, James RS, Ebens CL, Walter JM, Zijdenbos A, Evans AC, Giedd JN, Rapoport JL (2002): Developmental trajectories of brain volume abnormalities in children and adolescents with attention-deficit/hyperactivity disorder. JAMA 288:1740–1748.

Castellanos FX, Sonuga-Barke EJ, Milham MP, Tannock R (2006): Characterizing cognition in ADHD: Beyond executive dysfunction. Trends Cogn Sci 10:117–123.

Castellanos FX, Margulies DS, Kelly C, Uddin LQ, Ghaffari M, Kirsch A, Shaw D, Shehzad Z, Di Martino A, Biswal B, Sonuga-Barke EJ, Rotrosen J, Adler LA, Milham MP: Cingulate-precuneus interactions: A new locus of dysfunction in adult attention-deficit/hyperactivity disorder. Biol Psychiatry (in press).

Conover WJ (1980): Practical Nonparametric Statistics. 2nd Ed., John Wiley & Sons, NY.

Cox RW (1996): AFNI: Software for analysis and visualization of functional magnetic resonance neuroimages. Comput Biomed Res 29:162–173.

De Vico Fallani F, Astolfi L, Cincotti F, Mattia D, Marciani MG, Salinari S, Kurths J, Gao S, Cichocki A, Colosimo A, Babiloni F (2007): Cortical functional connectivity networks in normal and spinal cord injured patients: Evaluation by graph analysis. Hum Brain Mapp 28:1334–1346.

Dickstein SG, Bannon K, Xavier Castellanos F, Milham MP (2006): The neural correlates of attention deficit hyperactivity disorder: An ALE meta-analysis. J Child Psychol Psychiatry 47:1051–1062.

Durston S, Hulshoff Pol HE, Schnack HG, Buitelaar JK, Steenhuis MP, Minderaa RB, Kahn RS, van Engeland H (2004): Magnetic resonance imaging of boys with attention-deficit/hyperactivity disorder and their unaffected siblings. J Am Acad Child Adolesc Psychiatry 43:332–340.

Faraone SV, Sergeant J, Gillberg C, Biederman J (2003): The worldwide prevalence of ADHD: Is it an American condition? World Psychiatry 2:104–113.

Ferri R, Rundo F, Bruni O, Terzano MG, Stam CJ (2007): Small-world network organization of functional connectivity of EEG slow-wave activity during sleep. Clin Neurophysiol 118:449–456.

Fox MD, Snyder AZ, Vincent JL, Corbetta M, Van Essen DC, Raichle ME (2005): The human brain is intrinsically organized into dynamic, anticorrelated functional networks. Proc Natl Acad Sci USA 102:9673–9678.

Friston KJ, Frith CD, Liddle PF, Frackowiak RS (1993): Functional connectivity: The principal-component analysis of large (PET) data sets. J Cereb Blood Flow Metab 13:5–14.

Friston KJ, Frith CD, Frackowiak RS, Turner R (1995): Characterizing dynamic brain responses with fMRI: A multivariate approach. Neuroimage 2:166–172.

Gong YX, Cai TS (1993): Manual of Chinese revised Wechsler Intelligence Scale for Children (in Chinese). Changsha: Hunan Atlas Publishing House.

Greicius MD, Krasnow B, Reiss AL, Menon V (2003): Functional connectivity in the resting brain: A network analysis of the default mode hypothesis. Proc Natl Acad Sci USA 100:253–258.

Greicius MD, Flores BH, Menon V, Glover GH, Solvason HB, Kenna H, Reiss AL, Schatzberg AF (2007): Resting-state functional connectivity in major depression: Abnormally increased contributions from subgenual cingulate cortex and thalamus. Biol Psychiatry 62:429–437.

Hagmann P, Meuli R, Thiran J-P (2007): Mapping human whole-brain structural networks with diffusion MRI. PLoS ONE 2:e597.

He Y, Chen ZJ, Evans AC (2007): Small-world anatomical networks in the human brain revealed by cortical thickness from MRI. Cereb Cortex 17:2407–2419.

Hilgetag CC, Burns GA, O'Neill MA, Scannell JW, Young MP (2000): Anatomical connectivity defines the organization of clusters of cortical areas in the macaque monkey and the cat. Philos Trans R Soc Lond B Biol Sci 355:91–110.

Hill DE, Yeo RA, Campbell RA, Hart B, Vigil J, Brooks W (2003): Magnetic resonance imaging correlates of attention-deficit/hyperactivity disorder in children. Neuropsychology 17:496–506.

Honey CJ, Kotter R, Breakspear M, Sporns O (2007): Network structure of cerebral cortex shapes functional connectivity on multiple time scales. Proc Natl Acad Sci USA 104:10240–10245.

Hynd GW, Semrud-Clikeman M, Lorys AR, Novey ES, Eliopulos D, Lyytinen H (1991): Corpus callosum morphology in attention deficit-hyperactivity disorder: Morphometric analysis of MRI. J Learn Disabil 24:141–146.

Jiang T, He Y, Zang Y, Weng X (2004): Modulation of functional connectivity during the resting state and the motor task. Hum Brain Mapp 22:63–71.

Kaiser M, Hilgetag CC (2006): Nonoptimal component placement, but short processing paths, due to long-distance projections in neural systems. PLoS Comput Biol 2:e95.

Kiviniemi V, Jauhiainen J, Tervonen O, Paakko E, Oikarinen J, Vainionpaa V, Rantala H, Biswal B (2000): Slow vasomotor fluctuation in fMRI of anesthetized child brain. Magn Reson Med 44:373–378.

Kiviniemi V, Kantola JH, Jauhiainen J, Tervonen O (2004): Comparison of methods for detecting nondeterministic BOLD fluctuation in fMRI. Magn Reson Imaging 22:197–203.

Lago-Fernandez LF, Huerta R, Corbacho F, Siguenza JA (2000): Fast response and temporal coherent oscillations in small-world networks. Phys Rev Lett 84:2758–2761.

Latora V, Marchiori M (2001): Efficient behavior of small-world networks. Phys Rev Lett 87:198701.

Lee JS, Kim BN, Kang E, Lee DS, Kim YK, Chung JK, Lee MC, Cho SC (2005): Regional cerebral blood flow in children with attention deficit hyperactivity disorder: Comparison before and after methylphenidate treatment. Hum Brain Mapp 24:157–164.

Makris N, Biederman J, Valera EM, Bush G, Kaiser J, Kennedy DN, Caviness VS, Faraone SV, Seidman LJ (2007): Cortical thinning of the attention and executive function networks in adults with attention-deficit/hyperactivity disorder. Cereb Cortex 17:1364–1375.

Micheloyannis S, Pachou E, Stam CJ, Vourkas M, Erimaki S, Tsirka V (2006a): Using graph theoretical analysis of multi channel EEG to evaluate the neural efficiency hypothesis. Neurosci Lett 402:273–277.

Micheloyannis S, Pachou E, Stam CJ, Breakspear M, Bitsios P, Vourkas M, Erimaki S, Zervakis M (2006b): Small-world networks and disturbed functional connectivity in schizophrenia. Schizophr Res 87:60–66.

Murias M, Swanson JM, Srinivasan R (2007): Functional connectivity of frontal cortex in healthy and ADHD children reflected in EEG coherence. Cereb Cortex 17:1788–1799.

Nishikawa T, Motter AE, Lai YC, Hoppensteadt FC (2003): Heterogeneity in oscillator networks: are smaller worlds easier to synchronize? Phys Rev Lett 91:014101.

Ponten SC, Bartolomei F, Stam CJ (2007): Small-world networks and epilepsy: Graph theoretical analysis of intracerebrally recorded mesial temporal lobe seizures. Clin Neurophysiol 118:918–927.

Salvador R, Suckling J, Coleman MR, Pickard JD, Menon D, Bullmore E (2005a): Neurophysiological architecture of functional magnetic resonance images of human brain. Cereb Cortex 15:1332–1342.

Salvador R, Suckling J, Schwarzbauer C, Bullmore E (2005b): Undirected graphs of frequency-dependent functional connectivity in whole brain networks. Philos Trans R Soc Lond B Biol Sci 360:937–946.

Salvador R, Martinez A, Pomarol-Clotet E, Gomar J, Vila F, Sarro S, Capdevila A, Bullmore E (2008): A simple view of the brain through a frequency-specific functional connectivity measure. NeuroImage 39:279–289.

Schulz KP, Fan J, Tang CY, Newcorn JH, Buchsbaum MS, Cheung AM, Halperin JM (2004): Response inhibition in adolescents diagnosed with attention deficit hyperactivity disorder during childhood: An event-related FMRI study. Am J Psychiatry 161:1650–1657.

Seeley WW, Menon V, Schatzberg AF, Keller J, Glover GH, Kenna H, Reiss AL, Greicius MD (2007): Dissociable intrinsic connectivity networks for salience processing and executive control. J Neurosci 27:2349–2356.

Seidman LJ, Valera EM, Bush G (2004): Brain function and structure in adults with attention-deficit/hyperactivity disorder. Psychiatr Clin North Am 27:323–347.

Seidman LJ, Valera EM, Makris N (2005): Structural brain imaging of attention-deficit/hyperactivity disorder. Biol Psychiatry 57:1263–1272.

Semrud-Clikeman M, Filipek PA, Biederman J, Steingard R, Kennedy D, Renshaw P, Bekken K (1994): Attention-deficit hyperactivity disorder: Magnetic resonance imaging morphometric analysis of the corpus callosum. J Am Acad Child Adolesc Psychiatry 33:875–881.

Smith AB, Taylor E, Brammer M, Toone B, Rubia K (2006): Task-specific hypoactivation in prefrontal and temporoparietal brain regions during motor inhibition and task switching in medication-naive children and adolescents with attention deficit hyperactivity disorder. Am J Psychiatry 163:1044–1051.

Spencer T, Biederman J, Wilens TE, Faraone SV (1998): Adults with attention-deficit/hyperactivity disorder: A controversial diagnosis. J Clin Psychiatry 59(Suppl 7):59–68.

Sporns O, Tononi G (2002): Classes of network connectivity and dynamics. Complexity 7:28–38.

Sporns O, Zwi JD (2004): The small world of the cerebral cortex. Neuroinformatics 2:145–162.

Sporns O, Chialvo DR, Kaiser M, Hilgetag CC (2004): Organization, development and function of complex brain networks. Trends Cogn Sci 8:418–425.

Stam C, Reijneveld J (2007): Graph theoretical analysis of complex networks in the brain. Nonlin Biomed Phys 1:3.

Stam CJ (2004): Functional connectivity patterns of human magnetoencephalographic recordings: A 'small-world' network? Neurosci Lett 355:25–28.

Stam CJ, Jones BF, Nolte G, Breakspear M, Scheltens P (2007): Small-world networks and functional connectivity in Alzheimer's disease. Cereb Cortex 17:92–99.

Stephan KE, Hilgetag CC, Burns GA, O'Neill MA, Young MP, Kotter R (2000): Computational analysis of functional connectivity between areas of primate cerebral cortex. Philos Trans R Soc Lond B Biol Sci 355:111–126.

Strogatz SH (2001): Exploring complex networks. Nature 410:268–276.

Talairach J, Tournoux P (1998): Coplanar Stereotactic Atlas of the Human Brain. New York: Thieme Medical.

Tian L, Jiang T, Wang Y, Zang Y, He Y, Liang M, Sui M, Cao Q, Hu S, Peng M, Zhuo Y (2006): Altered resting-state functional connectivity patterns of anterior cingulate cortex in adolescents with attention deficit hyperactivity disorder. Neurosci Lett 400:39–43.

Toga AW, Thompson PM, Mori S, Amunts K, Zilles K (2006): Towards multimodal atlases of the human brain. Nat Rev Neurosci 7:952–966.

Tzourio-Mazoyer N, Landeau B, Papathanassiou D, Crivello F, Etard O, Delcroix N, Mazoyer B, Joliot M (2002): Automated anatomical labeling of activations in SPM using a macroscopic anatomical parcellation of the MNI MRI single-subject brain. Neuroimage 15:273–289.

Vaidya CJ, Austin G, Kirkorian G, Ridlehuber HW, Desmond JE, Glover GH, Gabrieli JD (1998): Selective effects of methylphenidate in attention deficit hyperactivity disorder: A functional magnetic resonance study. Proc Natl Acad Sci USA 95:14494–14499.

Wang L, Zang Y, He Y, Liang M, Zhang X, Tian L, Wu T, Jiang T, Li K (2006): Changes in hippocampal connectivity in the early stages of Alzheimer's disease: Evidence from resting state fMRI. Neuroimage 31:496–504.

Watts DJ, Strogatz SH (1998): Collective dynamics of 'small-world' networks. Nature 393:440–442.

Yang L, Wang Y, Qian Q, Gu B (2001): Primary exploration of the clinical subtypes of attention deficit hyperactivity disorder in Chinese children (in Chinese). Chin J Psychiatry 34:204–207.

Zang YF, He Y, Zhu CZ, Cao QJ, Sui MQ, Liang M, Tian LX, Jiang TZ, Wang YF (2007): Altered baseline brain activity in children with ADHD revealed by resting-state functional MRI. Brain Dev 29:83–91.